Research Article | Vol. 27, No. 17 | 19 Aug 2019 | OPTICS EXPRESS 24135
Optics EXPRESS

Power efficient optical frequency comb generation using laser gain switching and dual-drive Mach-Zehnder modulator

AMOL DELMADE,[1,*] MARKO KRSTIĆ,[2] COLM BROWNING,[1] JASNA CRNJANSKI,[2] DEJAN GVOZDIĆ,[2] AND LIAM BARRY[1]

[1]*Radio and Optical Communication Lab, School of Electronic Engineering, Dublin City University, Dublin, Ireland*
[2]*School of Electrical Engineering, University of Belgrade, Belgrade, Serbia*
[*]*amol.delmade2@mail.dcu.ie*

Abstract: We propose and experimentally demonstrate a power efficient dual-stage optical frequency comb using laser gain switching followed by a dual-drive Mach-Zehnder modulator (DD-MZM). The laser is initially gain switched at ~ 9.5 GHz and the resultant comb is then expanded using a dual-drive Mach-Zehnder modulator driven at ~ 19 GHz with signal amplitudes below 1.5 V. The setup generates an optical frequency comb, with 12 lines within 3 dB flatness, in a power efficient manner. Theoretical analysis is presented and verified through simulation and experimental results.

1. Introduction

Optical frequency combs (OFCs) have been used in many applications such as optical metrology [1], molecular gas spectroscopy [2], ultra-broadband optical coherent communications [3], datacenter interconnects [4] and RF photonics [5]. These applications demand different characteristics of the comb sources. Spectral flatness, tunable central wavelength, high side-comb suppression ratio (SCSR), flexible and stable comb spacing, fixed phase relations, low amplitude RF drive voltages and low implementation cost are some of the desirable criteria for different OFC applications. Optical comb sources with correlated comb lines can be generated using different techniques such as mode-locking of semiconductor lasers (MLL) [6], four-wave mixing (FWM) using fiber nonlinearities [7], gain switching of the lasers [8] and external electro-optic modulators (EOMs) [9]. The fixed length of the cavity in MLLs does not allow variable free spectral range (FSR) and accounts for increased system complexity, while the requirement for dispersion shifted fiber and difficulties associated with center wavelength tunability makes FWM based comb sources impractical for use in deployable systems [7]. Gain switched optical comb sources are gaining importance (especially for RF photonics applications such as millimeter wave generation [10]) because of their simple and cost-efficient architecture, precisely controlled channel spacing, high level of correlation between the comb lines and low phase noise [8] upon injection locking with low linewidth laser. The number of comb lines generated directly from a gain switched laser are limited by the laser's optical bandwidth and the frequency of the drive signal. When generating an OFC with a line spacing of around 12.5 GHz we can typically achieve six comb lines within 3 dB flatness [10]. To increase the number of comb lines, an electro-optic phase modulator (PM) driven at multiples of the modulator V_π (half-wave voltage of MZM), can be employed after the gain switched laser [8], and this technique has the potential to be integrated on a single chip.

Single or multiple external modulators in cascade can be used to generate FSR tunable comb sources [11–13], with a large number of comb lines. OFC generation using single phase modulator [9] typically provides poor spectral flatness and produces a limited number of comb

#367909 https://doi.org/10.1364/OE.27.024135
Journal © 2019 Received 24 May 2019; revised 23 Jul 2019; accepted 25 Jul 2019; published 8 Aug 2019

Optics EXPRESS

lines. To increase the number of comb lines generated it is normally necessary to either increase the RF power of the signal driving the modulator and/or use a cascade of modulators. Spectrally flat 11 comb lines have been generated by applying 10 GHz RF sinusoidal signal with ~ 40 V peak-to-peak voltage ($V \sim 7.38V_\pi$) to a dual-drive Mach-Zehnder modulator (DD-MZM) in [11], while 38 comb lines with a FSR of 25 GHz are obtained in [12] by applying ~ 20 V peak-to-peak ($V \sim 6.67V_\pi$) RF signal to a cascade of one intensity modulator (IM) and two PMs. Work presented in [13] achieved 21 comb lines with 25 GHz FSR by using two cascaded PMs with a 13 V ($V \sim 3.25V_\pi$) drive signal, followed by a third PM which had a frequency shifted signal applied to it. The required RF drive signal peak-to-peak voltage was reduced to ~ 6 V ($V \sim 1.054V_\pi$) for single drive by correctly biasing a dual parallel MZM appropriately to obtain 7 comb lines in [14], while in a recent simulation paper [15] the outputs of two polarization modulators biased at maximum and minimum transmission points, respectively, are combined to obtain 9 flat lines with an RF signal swing of < 4 V ($V \sim 0.97V_\pi$). As this previous work suggests, in order to design a power efficient comb source, an important requirement for these modulator-based comb sources is to reduce the RF drive signal to ensure high power RF amplifiers are not needed.

In previous work [8], we have demonstrated a wavelength tunable gain switched comb source by cascading a gain switched (GS) laser with a phase modulator to generate ~ 14-16 lines which are separated by 10 GHz. High RF drive voltage (~ 18 V, $V \sim 4.5V_\pi$) was required for comb line expansion using the PM. The RF drive level can be reduced by replacing the PM with a dual parallel MZM [14], polarization modulators [15] or a DD-MZM. With polarization modulators, polarization maintenance and the requirement for beam splitters leads to high system complexity, while adjusting the drift of the three modulator biases required for dual parallel MZM's can also become difficult. In this current work we use a DD-MZM for comb expansion. Simulation results show that cascading the gain switched laser with a DD-MZM biased at maximum transmission point and driven by an RF signal with twice the FSR frequency applied to the laser, can greatly increase the number of comb lines generated using a low drive voltage. In our experimental setup we use an RF drive voltage of less than 1.5 V (~ $0.586V_\pi$), which is applied to the DD-MZM to obtain 12 lines. This is substantially lower than previously presented results using EOM's for comb generation.

The paper is organized as follows. Section 2 presents the theoretical models of the gain switching and DD-MZM stage. Section 3 presents the experimental results. In Section 4, we give the comparison between experimental and theoretical results. The results are summarized in Section 5. Finally, in the appendix we give the fitting parameters used in the simulations.

2. Theoretical background

The scheme for power efficient frequency comb generation is based on the cascade of a gain switched laser and the DD-MZM stage, as shown in the Fig. 1. Gain switching of laser diode generates a comb of frequencies by driving the semiconductor laser with an electrical sinusoidal signal. It switches the laser diode from below, to above the lasing threshold and produces a sequence of optical pulses with a repetition frequency equal to the modulating frequency. In order to increase the number of comb lines obtained from the laser, its output signal is forwarded to the input of DD-MZM, which replicates the input comb pattern to higher and lower spectrum range.

2.1. Model of the gain switched laser

Our analysis shows that at the higher switching bias currents, the dynamics of the laser diode used in the experiment can be accurately described by the extended rate equations model which accounts for the carrier transport and parasitic effects [16,17]. This model provides more realistic small and large signal modulation response of the laser as well as the phase distortions of the emitted light, which is crucial for the shaping of the comb lines. We consider a multiple quantum

Optics EXPRESS

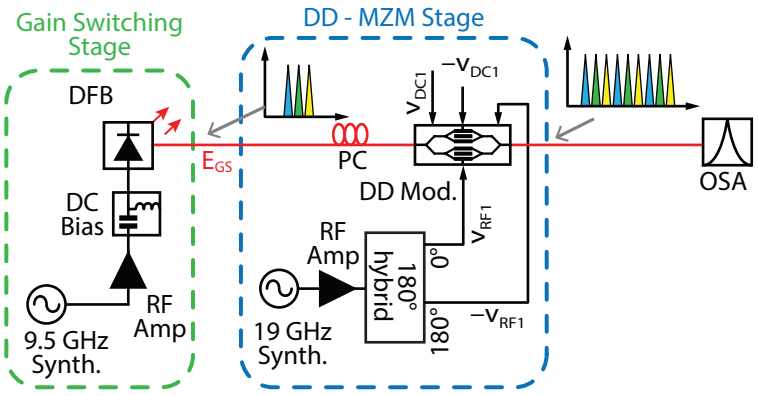

Fig. 1. Gain switching and DD-MZM based two-stage comb source.

well DFB laser and set the rate equations model as in [16], which follows the dynamics of the carrier density in the barrier (continuum) states (n_b), carrier density in the bound states of the well region (n_w), photon density (S) and the optical phase (ϕ):

$$\frac{dn_b}{dt} = \frac{\eta_{inj} I}{qV_{tot}} - \frac{n_b}{\tau_b} - \frac{n_b}{\tau_{bw}} + \frac{n_w V_w}{\tau_{wb} V_{tot}}. \tag{1}$$

$$\frac{dn_w}{dt} = \frac{n_b V_{tot}}{\tau_{bw} V_w} - \frac{n_w}{\tau_w} - \frac{n_w}{\tau_{wb}} - \frac{v_g \Omega (n_w - n_0) S}{1 + \varepsilon S}. \tag{2}$$

$$\frac{dS}{dt} = \frac{\Gamma v_g \Omega (n_w - n_0) S}{1 + \varepsilon S} - \frac{S}{\tau_p} + \Gamma \frac{R_{sp}}{V_{tot}}. \tag{3}$$

$$\frac{d\phi}{dt} = \frac{1}{2} \alpha \Gamma v_g \Omega (n_w - n_{th}). \tag{4}$$

In the equations above, η_{inj} is the injection efficiency, q stands for the elementary charge, I is the electrical bias current, while V_{tot} is the total volume of the separate confinement heterostructure (SCH) and the active region and V_w is the volume of the wells. Next, τ_b and τ_w are the carrier recombination lifetimes in the barrier and well region, respectively. The effective carrier diffusion across the SCH region and capture time by the wells is modeled by the "capture time" τ_{bw}, while the "escape time" τ_{wb} is the thermionic emission and carrier diffusion time from the well to the barrier states. Finally, parameter v_g stands for the group velocity of the light, Ω stands for the differential gain, n_0 for the transparency carrier density, S for the photon density, Γ for the optical confinement factor, τ_p for the photon lifetime, ε for the nonlinear gain suppression coefficient, R_{sp} for the spontaneous emission rate, α for the linewidth enhancement factor, and n_{th} for the threshold carrier density in the well region. Details about extracting parameters of commercially available laser used in experiment, and the parameter values used in simulation are given in Appendix A.

In the gain switching stage, the laser is driven by sinusoidal electrical current in the form $I(t) = I_{DC} + \Delta I \sin(2\pi f_{gs} t)$, where I_{DC} stands for the constant bias current, ΔI for the large amplitude, and f_{gs} for the frequency of the gain switching. The output complex electrical field of the gain switched laser E_{GS} is expressed as:

$$E_{GS}(t) = \sqrt{S(t)} e^{i\phi(t)}. \tag{5}$$

Flatness of the comb lines obtained in the gain switching stage is determined by the peak-to-peak amplitude of the electric field phase corresponding to emitted light.

Optics EXPRESS

2.2. DD-MZM model

The output complex electrical field after the DD-MZM stage E_{out} can be expressed as [18]:

$$E_{\text{out}} = \frac{1}{2} E_{\text{GS}}(t) \left[\exp(i\varphi_1(t)) + \exp(i\varphi_2(t))\right], \tag{6}$$

with E_{GS} standing for the complex electrical field generated by the gain switching process, while $\varphi_1(t)$ and $\varphi_2(t)$ stand for induced phases in the modulator arms, i.e.:

$$\varphi_1(t) = \frac{\pi}{V_\pi} v_1(t), \quad \varphi_2(t) = \frac{\pi}{V_\pi} v_2(t), \tag{7}$$

where $v_1(t)$, $v_2(t)$ represent voltages applied on each modulator arm. We analyze the case in which DD-MZM is driven by simple harmonic voltages in the form:

$$v_1(t) = V_{\text{DC}_1} + V_{\text{RF}_1} \cos(2\pi f_{\text{MZM}} t), \quad v_2(t) = V_{\text{DC}_2} + V_{\text{RF}_2} \cos(2\pi f_{\text{MZM}} t), \tag{8}$$

where V_{DC} and V_{RF} define the quiescent point and modulation depth for each modulator arm, respectively, while f_{MZM} denotes the frequency at which MZM is modulated. Substitution of Eqs. (7) and (8) in Eq. (6) gives:

$$E_{\text{out}}(t) = E_{\text{GS}}(t) \cos\left\{\frac{\pi}{2V_\pi}\left[v_1(t) - v_2(t)\right]\right\} \exp\left\{i\frac{\pi}{2V_\pi}\left[v_1(t) + v_2(t)\right]\right\}. \tag{9}$$

We operate DD-MZM in the push-pull configuration, so we have $v_1(t) = -v_2(t)$ i.e., $V_{\text{DC}_1} = -V_{\text{DC}_2}$ and $V_{\text{RF}_1} = -V_{\text{RF}_2}$. This gives pure intensity modulation, i.e., the original phase of E_{GS} stays preserved and Eq. (9) becomes:

$$E_{\text{out}}(t) = E_{\text{GS}}(t) \cos\left[\eta + \xi \cos(2\pi f_{\text{MZM}} t)\right], \tag{10}$$

with $\eta = \pi V_{\text{DC}_1}/V_\pi$ and $\xi = \pi V_{\text{RF}_1}/V_\pi$, where V_π denotes the switching bias voltage of the DD-MZM. Decomposing the cosine of the sum of two angles in the Eq. (10), and using Jacobi-Anger expansion, the last equation can be rewritten as:

$$\begin{aligned} E_{\text{out}}(t) = E_{\text{GS}}(t) &\left[\cos(\eta)\left(J_0(\xi) + 2\sum_{k=1}^{\infty}(-1)^k J_{2k}(\xi)\cos(2k2\pi f_{\text{MZM}} t)\right)\right] \\ &- E_{\text{GS}}(t)\left[\sin(\eta)\left(-2\sum_{k=1}^{\infty}(-1)^k J_{2k-1}(\xi)\cos((2k-1)2\pi f_{\text{MZM}} t)\right)\right], \end{aligned} \tag{11}$$

where J_k denotes Bessel function of the first kind. The equation shows that the electrical field obtained by the gain switching E_{GS} is further intensity modulated with harmonics which are weighted with Bessel function values, in a way that even harmonics are weighted by even order Bessel functions, while odd harmonics are weighted by odd order Bessel functions. By setting the quiescent point, i.e., factor η, even or odd harmonics could be suppressed, provided that $\cos(\eta) = 0$ or $\sin(\eta) = 0$.

In the gain switching stage, by using rate equations model given by Eqs. (1)-(4) and parameter values extracted from fitting the commercially available laser used in experiment, we produce a comb with 3 flat lines with FSR corresponding to the gain switching frequency f_{gs} as schematically depicted in Fig. 2. The same results can be achieved with simpler model [19], which does not include parasitic-like effects, since the number of comb lines is limited by extracted linewidth enhancement factor α in case of fixed bias current. Regardless of the rate equation model used, the model of the gain switched laser which assumes a simple trigonometric periodic function

Optics EXPRESS

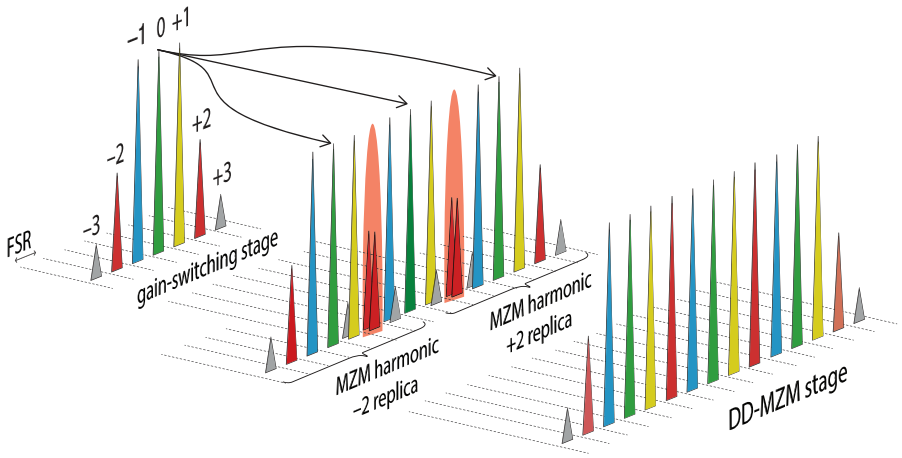

Fig. 2. The schematic concept of the gain switched comb expansion. Three flat lines frequency comb generated after the gain switching stage. The symmetrical distribution of the side-comb lines (lines ±2) is feasible for simple harmonic optical phase modulation profile. Expansion of the comb after the DD-MZM stage. MZM harmonics ±2 produce spectrum replicas which contribute to expansion of the final comb to 11 flat lines. The arrowed lines depict the directions of mappings between the original spectrum and its replicas due to MZM expansion. Flatness of the expanded comb crucially depends on the summation of the lines −2 and +2 between original spectrum and its replicas.

of phase time-dependence (sine/cosine), leads to the symmetric distribution of the comb lines around the fundamental comb frequency (central line, denoted with 0 in the Fig. 2). In addition to several equalized combs lines (in our case 3, denoted with 0 and ±1), there are some other side-comb lines with lower intensities (±2, ±3,...), which decay as the frequency separation from the fundamental comb line increases.

These side-combs lines with lower intensity, especially the first one closest to the group of flat lines (±2 in Fig. 2), might contribute to generation of additional combs. The original optical phase of the gain switching stage comb is preserved, while the amplitude of the corresponding electrical field is modulated by MZM harmonics as given by Eq. (11). The result of applied configuration is that MZM harmonics provide the frequency shift of the input comb spectrum obtained by the gain switched laser and generate its replicas at higher and lower frequency range, preserving the original set of comb lines (Fig. 2). In the proposed scheme, we use only even MZM harmonics by setting $V_{\mathrm{DC}_1} = V_\pi$ and $V_{\mathrm{DC}_2} = -V_\pi$ which makes $\eta = \pi$, consequently $\sin(\eta) = 0$ and eliminates the odd MZM harmonics from Eq. (11). Moreover, we set the RF voltage to equate the power of the fundamental MZM harmonic with the first even MZM harmonic (i.e., MZM harmonic ±2), by equating the corresponding Bessel functions $|J_0(\xi)| = |J_2(\xi)|$. This is feasible for $\xi = 0.586\pi$ i.e., $V_{\mathrm{RF}_1} = 0.586V_\pi$. In this case higher even MZM harmonics (i.e., MZM harmonics ±4, ±6,...) are significantly suppressed as the values of the higher Bessel functions $J_4(\xi)$, $J_6(\xi)$,... are approximately zero. In order to replicate the laser comb spectrum and to shift it to the edges of its frequency range, we modulate the MZM by modulation frequency f_{MZM} which shifts the replicas of the spectrum by $4f_{\mathrm{gs}}$. Since we use the second MZM harmonic, the necessary frequency of the MZM modulation is given by $f_{\mathrm{MZM}} = 4f_{\mathrm{gs}}/2 = 2f_{\mathrm{gs}}$. In this way, the spectrum replica originating from the MZM harmonic −2, produces the overlapping of the side-comb line +2 from the spectrum replica, with the side-comb line −2 from the original spectrum (overlapping of the two red comb lines shown in the Fig. 2). On the other side, the spectrum replica originating from the MZM harmonic +2, produces the overlapping of the

Optics EXPRESS

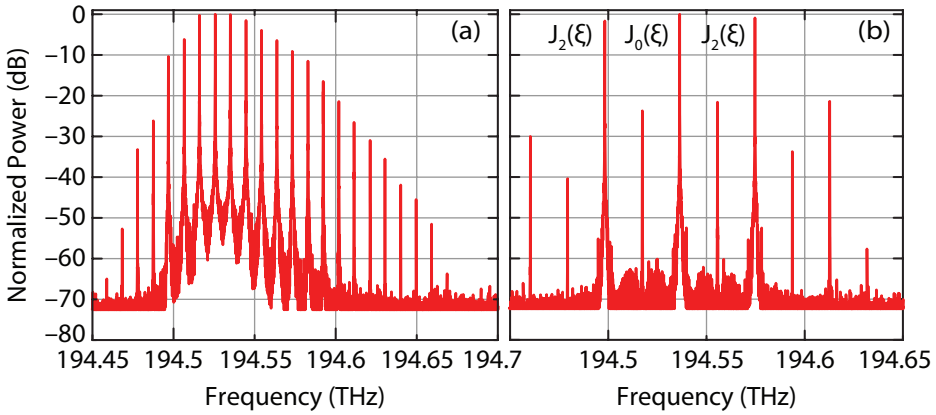

Fig. 3. (a) Measured gain switched laser output spectrum with FSR of around 9.5 GHz. Three flat comb lines are obtained within 1 dB of flatness. (b) DD-MZM output spectrum for CW input. MZM driving voltage is set to suppress odd MZM harmonics and to equate the fundamental MZM harmonic with the first even harmonic, by setting $|J_0(\xi)| = |J_2(\xi)|$ (Eq. (11)).

side-comb line −2 from the spectrum replica, with the side-comb line +2 from the original spectrum. The final comb consists of $3 \times 3 = 9$ flat lines as the result of direct replicas of the initial spectrum, plus 2 additional lines as the result of the overlapping. In the case in which overlapping produces comb lines with similar power to the initially flat ones, the final comb can be comprised of 11 flat comb lines.

However, the presented concept assumes perfect simple periodic phase dependence on time, which is distorted and strongly affected by the carrier transport and parasitic effects in the case of higher modulation depths. In this case, the extended rate equations model given by Eqs. (1)-(4) may account for phase distortion, leading to asymmetry of the spectrum, which further modifies the number of flat comb lines which might be smaller or larger than 11, depending on the superposition of replicated comb lines. This problem will be discussed in the section dealing with comparison of experiment and theory.

3. Experimental results

The schematic configuration of our two-stage comb source generation is depicted in Fig. 1. The gain switching stage is depicted in the green framed box in Fig. 1, while the blue framed box in Fig. 1 depicts the DD-MZM stage. In the gain switching stage, a commercially available distributed feedback (DFB) laser, which is packaged in an optically un-isolated temperature controlled high-speed butterfly package, emitting the light in the 1.5 μm window, is used. The small signal modulation bandwidth was measured to be around 19 GHz, at the room temperature, when biased at $4I_{\text{th}}$. The laser is gain switched at $f_{\text{gs}} \sim 9.5$ GHz using an amplified RF signal with a power of ~ 18 dBm, corresponding to peak-to-peak bias current of $2\Delta I \approx 100$ mA. The steady-state bias current of $I_{\text{DC}} = 67.5$ mA is used. This results in coherent optical tones with an FSR of ~ 9.5 GHz as shown in the optical spectrum of Fig. 3(a). Three flat lines are obtained within less than 1 dB flatness as seen from the spectrum shown in Fig. 3(a) (comb lines 0, +1 and −1) with a carrier to noise ratio of ~ 45 dB. An increased number of lines can be obtained by gain switching with increased RF signal power and/or reduced laser bias current [10], but will result in the reduction of the carrier to noise ratio.

The output of the gain switching stage is then connected to the DD-MZM through a polarization controller (PC) (as shown in Fig. 1). A 30 GHz dual drive modulator from Fujitsu with a V_π of

Optics EXPRESS

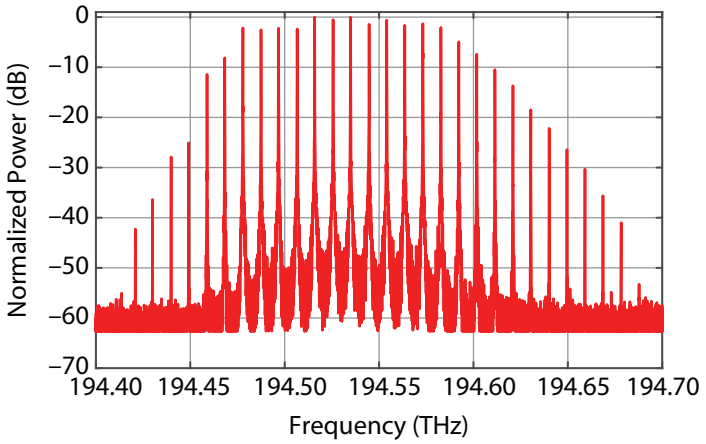

Fig. 4. Two-stage comb source output spectrum with 12 lines in 3 dB flatness and FSR of 9.5 GHz.

2.5 V is biased at the maximum transmission point ($V_{DC} = V_\pi$) to suppress odd harmonics and generate only the even harmonics, represented by Eq. (11) and as explained in the Section 2.2. 0° and 180° phase shifted 19 GHz ($f_{MZM} = 2f_{gs} = 19$ GHz) sinusoidal signals are applied to either arm of the DD-MZM (as shown in Fig. 1) after suitable amplification to achieve the required drive signal with a peak voltage of $V_{RF} \approx 1.46$ V ($0.586V_\pi$). For CW laser operation, these biasing and modulation conditions result in suppression of odd harmonics and $|J_0(\xi)| = |J_2(\xi)|$ as can be seen from the DD-MZM output spectrum shown in Fig. 3(b). Odd harmonic frequencies are suppressed by ~ 23 dB, approximately the same as the extinction ratio of the modulator. These three flat even harmonics from the DD-MZM, are separated by around 38 GHz ($2 \times 2f_{MZM}$) from each other as shown in Fig. 3(b).

Fig. 4 presents the results of our experiment and shows the output spectrum of the dual stage comb source when both gain switching laser and DD-MZM are under modulation with above mentioned conditions. Twelve lines within ~ 3 dB flatness, constituting a total bandwidth of ~ 105 GHz, are obtained with an FSR of ~ 9.5 GHz and a carrier to noise ratio of ~ 42 dB. These experimental results essentially follow our theoretical analysis given in the Section 2.2. The discrepancy between theoretical prediction and experimental results, will be explained in the next section dealing with their comparison. A sinusoidal signal of ~ 1.46 V peak amplitude is required to obtain twelve flat lines, compared to 18 V required for PM in [8] making this scheme power efficient.

4. Comparison of theoretical and experimental results

By the means of our rate equations model given by Eqs. (1)-(4), we simulate the gain switching process by driving the laser with large-amplitude bias current almost exactly the same as in the experiment with steady-state bias current of $I_{DC} = 67.5$ mA and peak-to-peak current of $\Delta I = 105$ mA. In Fig. 5(a) we present the obtained optical frequency comb at the gain switching stage, as the result of Fourier transformation of Eq. (5). The relative frequency is given with respect to the central comb line, corresponding to the central lasing frequency (194.5371 THz). The simulated comb has three lines (lines −1, 0, and 1, corresponding to −9.5, 0, and 9.5 GHz, respectively) within around 2 dB flatness, denoted with solid blue dots. With red solid line we depict the envelope of the experimentally measured comb, given in Fig. 3(a), exhibiting high agreement with our simulation results. It should be emphasized that the rate equations model which does not include the parasitic-like effects, is not able to account for phase distortion,

Optics EXPRESS

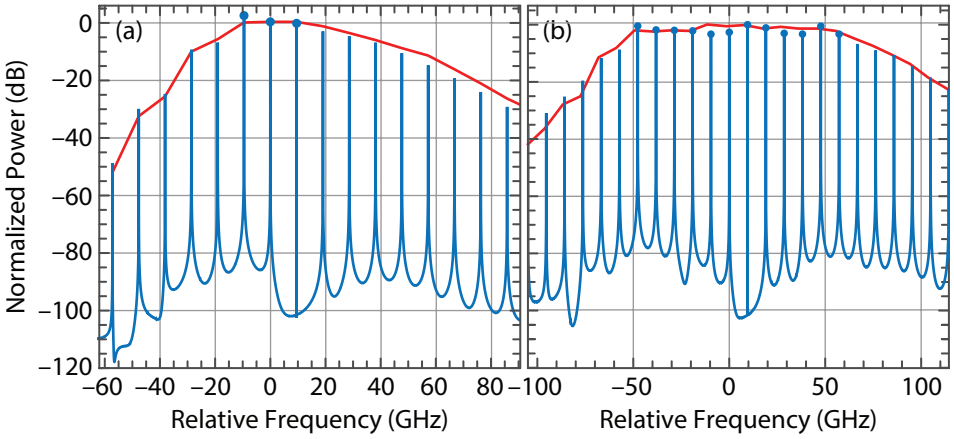

Fig. 5. (a) Simulated gain-switched laser output spectrum with three lines in 2 dB flatness (blue dots). Red solid line stands for the experimentally measured comb envelope, showing an excellent agreement with simulation. (b) Simulated DD-MZM output spectrum with 12 lines in 3 dB flatness (blue dots), obtained with low MZM RF voltage ($V_{RF} = 0.586V_\pi$). Red solid line stands for the experimentally measured comb envelope, showing an excellent agreement with simulation.

causing the laser spectrum asymmetry noticeable in the experimental results. However, the implementation of the extended rate equation model of the gain switched laser accounting for carrier transport as well as capture and escape effects, provides excellent fit of the experimentally measured data.

In the next stage, the DD-MZM is biased in the push-pull configuration with RF voltage set to equate the first even MZM harmonic with the fundamental one, while suppressing the others by means of the Fourier transform of Eq. (11) with $\eta = \pi$, $\xi = 0.586\pi$ and $f_{MZM} = 2f_{gs} = 19$ GHz. The simulation leads to an expanded comb depicted in Fig. 5(b). It provides 12 lines within 3 dB of flatness, denoted with blue dots. Again, with the red line we depict the envelope of the experimentally measured comb as given in Fig. 4, to emphasize extremely good matching of our simulation with the measured data. The number of comb lines obtained by experiment and simulation (12) is increased in comparison with conceptually predicted number (11). The reason for discrepancy is the nonlinear phase distortion and corresponding laser spectrum asymmetry, which occurs due to deep gain switching and parasitic-like effects affecting the phase time dependence. The asymmetry of the spectrum causes the difference in magnitude of the side combs ±2 and consequently redistribution of the comb magnitudes mixing at the output of DD-MZM. Indeed, the lines −2 and +2 in the gain switching spectrum are not symmetrical in intensity, the line +2 is significantly stronger, moreover, in 3 dB margin with the three flat lines (lines −1, 0, and 1). Still, overlapping of the lines −2 and +2 schematically depicted in the Fig. 2, produces lines comparable to the three initially flat lines and their replicas, in this way forming the spectrum with 11 flat lines, as discussed in the Section 2.2. However, the line +2 from the spectrum replica originating from the MZM harmonic +2 emerges as the 12th flat line, since it is in 3 dB margin with the three flat lines in the gain switching spectrum. The result in this case is finally favorable, although the distortion could lead to decrease of comb line number or reduction of the line flatness.

It should be noted that $\xi \approx 3.14\pi$ i.e., $V_{RF_1} \approx 3.14V_\pi$ (corresponding in this case to $V_{RF_1} \approx 7.85$ V) could yield $|J_0(\xi)| \approx |J_2(\xi)|| \approx |J_4(\xi)|$ which could add two more replicas originating from the MZM harmonics ±4. In this case our simulations give 20 lines in around 3.8 dB flatness. The conceptual approach predicts 19 lines corresponding to 5 replicas of the

Optics EXPRESS

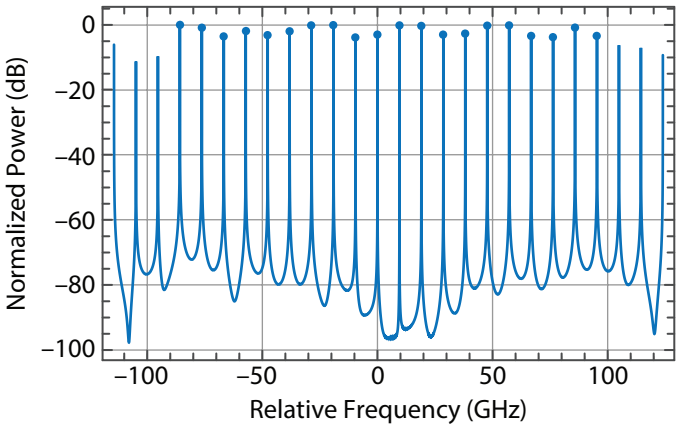

Fig. 6. Simulated DD-MZM output spectrum with 20 lines in 3.8 dB flatness (blue dots), obtained with higher MZM RF voltage ($V_{\mathrm{RF_1}} \approx 3.14V_\pi$).

initially 3 flat lines, plus 2 lines resulting from overlapping of the original spectrum with second MZM harmonic, 2 lines resulting from overlapping of the second and fourth MZM harmonic. The additional line is due to the gain-switched spectrum asymmetry, i.e., due to the pronounced +2 line from the spectrum replica originating from the MZM harmonic +4, which finally gives $5 \times 3 + 2 + 2 + 1 = 20$ lines as shown in the Fig. 6. Although it is effective with respect to the generation of large number of comb lines, this scheme needs higher RF voltage applied to the MZM arms. Since in this paper we focus on the power efficient comb generation, we will investigate proposed method and further optimizations to improve the line flatness in future publications. In addition to that, we will study reduction of laser bias current, which as shown in [9] can yield higher number of comb lines (6) even in the first stage of the scheme.

5. Conclusion

In this paper we demonstrate a power efficient method for the generation of an optical frequency comb by cascading a gain switched laser and dual-drive Mach-Zehnder modulator, operated in the push-pull configuration. In the gain switching stage we generate a 9.5 GHz free spectral range frequency comb with three flat comb lines, by direct large-signal modulation of a DFB laser diode. We further expand the comb by using a dual-drive Mach-Zehnder modulator driven at 19 GHz ($2 \times$ FSR) with signal amplitudes below 1.5 V, which due to suppression of odd frequencies, and second harmonic generation corresponding to 4-fold FSR shift, making the proposed scheme highly power efficient. The expanded comb consists of 12 lines within 3 dB flatness. The model of gain switched lasers based on extended rate equations accounting for parasitic-like effects can grasp the nonlinear phase distortion providing asymmetry of the laser spectrum and finally excellent agreements of the theoretically predicted and measured number of comb lines.

APPENDIX A. Laser parameters and fitting

From the extended rate equations system given by Eqs. (1)-(4), neglecting the spontaneous emission coupling term, for the small-signal electrical bias current, the normalized modulation response can be derived as in [16]:

$$\frac{M(\omega)}{M(0)} = \frac{\omega_r^2}{(1 + i\omega\tau_{\mathrm{bw}})(\omega_r^2 - \omega^2 + i\omega\gamma)}, \tag{12}$$

Optics EXPRESS

with:

$$\omega_r^2 = \frac{v_g(\Omega/\chi)}{\tau_p}\frac{S_0}{1+\varepsilon S_0}\left(1+\frac{\varepsilon}{v_g\Omega\tau_w}\right) \tag{13}$$

$$\gamma = v_g(\Omega/\chi)\frac{S_0}{1+\varepsilon S_0} + \frac{\varepsilon S_0}{\tau_p(1+\varepsilon S_0)} + \frac{1}{\chi\tau_w} \tag{14}$$

$$\chi = 1 + \frac{\tau_{bw}}{\tau_{wb}}. \tag{15}$$

In the equations above, the parameter χ models the influence of the parasitic effects which effectively reduce the differential gain, defining the effective differential gain $\Omega' = \Omega/\chi$. The capture time τ_{bw} is a constant which contributes to low-frequency roll-off, which is present in the experimentally measured modulation response curve, and S_0 stands for the steady-state photon density. In addition to equations above, we use standard linear dependence of output power on the applied bias current above the threshold ($P-I$ characteristic) [17] and standard relation between output power P and output photon density S [17], respectively:

$$P = \eta_d\frac{\hbar\omega_0}{q}(I - I_{th}), \tag{16}$$

$$S = \frac{\tau_p\Gamma P}{\eta_0 V_w\hbar\omega_0}, \tag{17}$$

where $\eta_d = \eta_{inj}\eta_0$ stands for the differential quantum efficiency [17], given as the product of the injection efficiency and optical efficiency, ω_0 for the angular frequency corresponding to the lasing central frequency f_0, and I_{th} for the threshold bias current.

Using relations (12)-(17) with measured $P-I$ curve and small-signal normalized modulation response at $I = 4I_{th}$, we fit laser parameters and by the means of our rate equations model given by Eqs. (1)-(4) we almost exactly reproduce the measured data. In the Table 1 we give laser fitting parameters' values used in the simulations, which are in the range expected for high-speed multiple quantum-well lasers [16, 17]. In Figs. 7(a) and 7(b) we show measured (red dotted lines) and simulation reproduced (blue solid lines) $P-I$ and small-signal normalized modulation response curves, respectively.

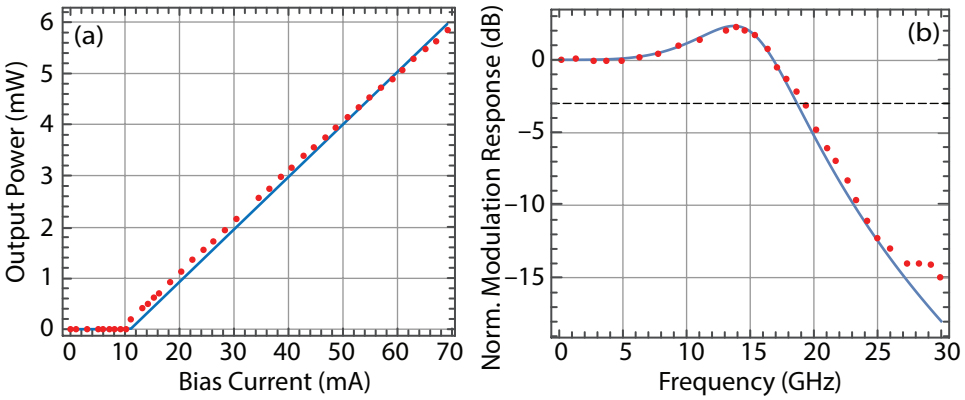

Fig. 7. Measured (red dots) and simulated (blue solid line) (a) $P-I$ curve and (b) small-signal normalized modulation response, obtained at $I = 4I_{th}$. Dashed line stands for −3 dB grid line.

Optics EXPRESS

Table 1. **Fitting parameters with their values used in the simulation**

Parameter		Value
Injection efficiency	η_{inj}	0.85
Total volume	V_{tot}	1.03×10^{-10} cm^3
Volume of wells	V_w	1.68×10^{-11} cm^3
Carrier lifetime in the well region	τ_w	2.5 ns
Carrier lifetime in the barrier region	τ_b	1.5 ns
Capture time	τ_{bw}	14.5 ps
Escape time	τ_{wb}	70 ps
Effective differential gain	$\Omega' = \Omega/\chi$	1.24×10^{-15} cm^2
Photon lifetime	τ_p	2.3 ps
Nonlinear gain suppression coefficient	ε	2×10^{-17} cm^4
Optical confinement factor	Γ	0.08
Carrier transparency density	n_0	4.2×10^{18} cm^{-3}
Spontaneous emission rate	R_{sp}	1.18×10^{12} s^{-1}
Linewidth enhancement factor	α	3.5
Group velocity	v_g	8.5×10^9 cm/s
Differential quantum efficiency	η_d	0.13
Lasing central frequency	f_0	194.5371 THz

Funding

SFI US-Ireland (15/US-C2C/I3132); CONNECT (13/RC/2077); IPIC (12/RC/2276); Serbian Ministry of Education, Science and Technological Development (ON171011, "Photonics Components and Systems").

References

1. T. Udem, R. Holzwarth, and T. W. Hansch, "Optical frequency metrology," Nature **416**(6877), 233–237 (2002).
2. V. Gerginov, C. E. Tanner, S. A. Diddams, A. Bartels, and L. Hollberg, "High resolution spectroscopy with a femtosecond laser frequency comb," Opt. Lett. **30**(13), 1734–1736 (2005).
3. A. D. Ellis and F. C. G. Gunning, "Spectral density enhancement using coherent WDM," IEEE Photonics Technol. Lett. **17**(2), 504–506 (2005).
4. V. T. Company and A. M. Weiner, "Optical frequency comb technology for ultra-broadband radio frequency photonics," Laser and Photonics Rev. **8**(3), 368–393 (2014).
5. Qixiang Cheng, Meisam Bahadori, Madeleine Glick, Sébastien Rumley, and Keren Bergman, "Recent advances in optical technologies for data centers: a review," Optica **5**(11), 1354–1370 (2018).
6. A. Akrout, A. Shen, R. Brenot, F. V. Dijk, O. Legouezigou, F. Pommereau, F. Lelarge, A. Ramdane, and G.-H. Duan, "Error-free transmission of 8 WDM channels at 10 Gbit/s using comb generation in a quantum dash-based mode-locked laser," in Proceedings of 34th European Conference on Optical Communication, Brussels, 21-25 Sept. 2008.
7. G. A. Sefler and K.-I. Kitayama, "Frequency comb generation by four-wave mixing and the role of fiber dispersion," J. Light. Technol. **16**(9), 1596–1605 (1998).

Optics EXPRESS

8. R. Zhou, S. Latkowski, J. O'Carroll, R. Phelan, L. P. Barry, and P. Anandarajah, "40nm wavelength tunable gain-switched optical comb source," in Proceedings of 37th European Conference and Exhibition on Optical Communication, Geneva, 18-22 Sept. 2011.
9. W. T. Wang, J. G. Liu, W. H. Sun, W. Chen, and N. H. Zhu, "Multi-band local microwave signal generation based on an optical frequency comb generator," Elsevier Opt. Commun. **338**, 90–94 (2015).
10. C. Browning, H. H. Elwan, E. P. Martin, S. O'Duill, J. Poette, P. Sheridan, A. Farhang, B. Cabon, and L. P. Barry, "Gain-switched optical frequency combs for future mobile radio-over-fiber millimeter-wave systems," J. Light. Technol. **36**(19), 4602–4610 (2018).
11. T. Sakamoto, T. Kawanishi, and M. Izutsu, "Widely wavelength-tunable ultra-flat frequency comb generation using conventional dual-drive Mach-Zehnder modulator," Electron. Lett. **43**(19), 1039–1040 (2007).
12. R. Wu, V. R. Supradeepa, C. M. Long, D. E. Leaird, and A. M. Weiner, "Generation of very flat optical frequency combs from continuous-wave lasers using cascaded intensity and phase modulators driven by tailored radio frequency waveforms," Opt. Lett. **35**(19), 3234–3236 (2010).
13. J. Zhang, J. Yu, N. Chi, Z. Dong, X. Li, Y. Shao, J. Yu, and L. Tao, "Flattened comb generation using only phase modulators driven by fundamental frequency sinusoidal sources with small frequency offset," Opt. Lett. **38**(4), 552–554 (2013).
14. Q. Wang, L. Huo, Y. Xing, and B. Zhou, "Ultra-flat optical frequency comb generator using a single-driven dual-parallel Mach-Zehnder modulator," Opt. Lett. **39**(10), 3050–3053 (2014).
15. R. B. Chaudhuri and A. D. Barman, "Generation of an optical frequency comb based on two cascaded dual-parallel polarization modulators," Appl. Opt. **57**(30), 9164–9171 (2018).
16. T. Keating, X. Jin, S. L. Chuang, and K. Hess, "Temperature dependence of electrical and optical modulation responses of quantum-well lasers," IEEE J. Quantum Electron. **35**(10), 1526–1534, (1999).
17. L. Coldren, S. Corzine, M. Mašanović, *Diode Lasers and Photonic Integrated Circuits* (John Wiley and Sons, 2012).
18. G. Agrawal, *Fiber-optic Communication Systems* (John Wiley and Sons, 2010).
19. S. L. Chuang, *Physics of Photonic Devices*, (John Wiley and Sons, 2012).